Latin American Journal of Solids and Structures
www.lajss.org

Improved high order free vibration analysis of thick double curved sandwich panels with transversely flexible cores

Abstract
This paper dealt with free vibration analysis of thick double curved composite sandwich panels with simply supported or fully clamped boundary conditions based on a new improved higher order sandwich panel theory. The formulation used the first order shear deformation theory for composite face sheets and polynomial description for the displacement field in the core layer which was based on the displacement field of Frostig's second model. The fully dynamic effects of the core layer and face sheets were also considered in this study. Using the Hamilton's principle, the governing equations were derived. Moreover, effects of some important parameters like that of boundary conditions, thickness ratio of the core to panel, radii curvatures and composite lay-up sequences were investigated on free vibration response of the panel. The results were validated by those published in the literature and with the FE results obtained by ABAQUS software. It was shown that thicker panels with a thicker core provided greater resistance to resonant vibrations. Also, effect of increasing the core thickness in general was significant decreased fundamental natural frequency values.

Keywords
Free vibration, Double curved sandwich panel, Boundary conditions, Improved higher order sandwich panel theory.

K. Malekzadeh Fard [a] *
M. Livani [a]
Faramarz Ashenai Ghasemi [b]

[a] Department of Structural Analysis and Simulation, Space Research Institute, Malek Ashtar University of Technology, Tehran-Karaj Highway, Post box: 13445-768, Tehran, Iran
m_livani@mut.ac.ir
[b] Department of Mechanical Engineering, Shahid Rajaee Teacher Training University (SRTTU), Lavizan, Postal Code 16788-15811,Tehran, Iran.
F.a.ghasemi@srttu.edu

*Author email: kmalekzadeh@mut.ac.ir

Received 04.03.2014
In revised form 06.06.2014
Accepted 11.06.2014
Available online 26.09.2014

1 INTRODUCTION

Structural efficiency is an important attribute for aircraft structures. A higher order theory approach, used by Kant and Patil (1991), replaced sandwich structure with an equivalent higher order shear deformable structure, which lacked the ability to determine local buckling modes and imperfection effects on the overall behavior. Using the three-dimensional elasticity equations, Bhimaraddi (1993) studied the static response of orthotropic doubly curved shallow shells. He assumed that the ratio of the shell thickness to its middle surface radius is negligible as compared to unity. The higher order sandwich panel theory was developed by Frostig *et al.* (1994, 2004), who considered two types of computational models in order to express governing equations of the core layer. The second model assumed a polynomial description of the displacement fields in the core that was based on displacement fields of the first model. Their theory did not impose any restrictions on distribution of the deformation through thickness of the core. Singh (1999) studied free vibration of the open deep sandwich shells made of thin layers and a moderately thick core. Rayleigh–Ritz method was also used to obtain natural frequencies. The improved higher order sandwich plate theory (IHSAPT), applying the first-order shear deformation theory for the face sheets, was introduced by Malekzadeh *et al.* (2005, 2006).

NOTATIONS

dV_t, dV_c, dV_b	Volume element of the top face sheet, the core and the bottom face sheet, respectively
I_n^i $(i = t,b,c)$	The moments of inertia of the top and bottom face sheets and the core
M_z^c	Normal bending moments per unit length of the edge of the core
$M_{xy}^i, M_{yx}^i, M_{xx}^i, M_{yy}^i$	Bending and shear moments per unit length of the edge (i=t,b)
$M_{nxx}^c, M_{nxy}^c, M_{nyy}^c, M_{nyx}^c$ $M_{nxz}^c, M_{nyz}^c, M_{nxz}^{*c}, M_{nyz}^{*c}$	Shear and bending moments per unit length of the edge of the core, (n=1,2,3)
$\bar{N}_{xxj}^i, \bar{N}_{yyj}^i, \bar{N}_{xyj}^i$	The in-plane external loads in the longitudinal and transverse direction, respectively (i = t, b), (j=1,2)
$N_{xy}^i, N_{yx}^i, N_{xx}^i, N_{yy}^i$	In-plane and shear forces per unit length of the edge (i=t,b)
$N_{xz}^c, N_{yz}^c, N_{xz}^{*c}, N_{yz}^{*c}$	Shear forces per unit length of the edge of the core
$N_{xxj}^i, N_{yyj}^i, N_{xyj}^i$	In plane resultant forces due to pre stresses (j=t,b)
Q_{ij}	The reduced stiffnesses referred to the principal material coordinates
$\bar{Q}_{ij}$	Transformed reduced stiffnesses
$R_{ix},\ R_{iy}$	Curvature radii of the top face sheet, bottom face sheet and core in x-z and y-z planes (i=t,b,c)
u_k, v_k, w_k	Unknowns of the in-plane displacements of the core (k=0,1,2,3)
u_c, v_c, w_c	Displacement components of the core
u_0^i, v_0^i, w_0^i	Displacement components of the face sheets, (i = t, b)
$\ddot{u}_c, \ddot{v}_c, \ddot{w}_c$	Acceleration components of the core
$\ddot{u}_{0j}, \ddot{v}_{0j}, \ddot{w}_{0j}$	Acceleration components of the face sheets, (j= t, b)
z_t , z_b ,z_c	Normal coordinates in the mid-plane of the top and the bottom face sheets and the core

GREEK LETTERS

ρ_t, ρ_b, ρ_c	Material densities of the face sheets and the core
σ_{ii}^{j}	Normal stress in the face sheets, (i=x,y), j=(t,b)
σ_{ii}^{c}	Normal stress in the core, (i=x,y,z)
$\tau_{xy}^{j}, \tau_{xz}^{j}, \tau_{yz}^{j}$	Shear stress in the face sheets, j=(t,b)
$\tau_{xy}^{c}, \tau_{xz}^{c}, \tau_{yz}^{c}$	Shear stresses in the core
$\varepsilon_{0xx}^{i}, \varepsilon_{0xy}^{i}, \varepsilon_{0yy}^{i}, \varepsilon_{0xz}^{i}, \varepsilon_{0xz}^{i}$	The mid-plane strain components, (i=t,b)
$\varepsilon_{zz}^{c}, \varepsilon_{xx}^{c}, \varepsilon_{yy}^{c}$	Normal strains components of the core layer
$\gamma_{xz}^{c}, \gamma_{yz}^{c}, \gamma_{xy}^{c}$	Shear strains components of the core layer
ψ_x^i, ψ_y^i	Rotation of the normal section of midsurface of the top face sheet and bottom face sheet along x and y, respectively(i=t,b)

Zenkour (2005a, b) presented a comprehensive bending, buckling and free vibration analysis of simply supported functionally graded (FG) ceramic–metal sandwich plates. The sandwich plate face sheets were assumed to be isotropic material. Two-constituent material distribution through thickness was assumed to vary according to a power law distribution. Garg *et al.* (2006) investigated free vibration analysis of simply supported composite and sandwich doubly curved shells. Their formulation included Sander's theory based on equivalent single layer approach. Free vibration of FG material sandwich rectangular plates with simply supported and clamped edges was studied by Li *et al.* (2008). The governing equations based on the three-dimensional linear theory of elasticity were derived and also they considered two common types of FG sandwich plates, namely sandwich plate with FG face sheets and homogeneous core and sandwich plate with homogeneous face sheets and FG core.

Experimental and analytical investigations of bending and free vibration response of layered FG beams were carried out by Kapuria *et al.* (2008), who demonstrated capability of the zigzag theory in modeling mechanics of such beams. Rahmani *et al.* (2009) studied free vibration analysis of open single curved composite sandwich panel with a flexible core using a higher order sandwich panel theory. Their formulation used classical shell theory for the face sheets and an elasticity theory for the core layer. Cetkovic and Vuksanovic (2009) investigated global and local responses of laminated and sandwich structures using Reddy's theory, finite element solution and based on equivalent single layer approach. Biglari and Jafari (2010a) presented a simple three layer theory in order to study vibration and static analysis of open single curved sandwich structures. In their model, they used Donell's theory for the face sheets and considered inconsistent linear stress variation in the core layer. They (2010b) also studied the free vibrations of doubly curved sandwich shell with flexible core based on a refined general-purpose sandwich panel theory. In their theory, the in-plane stresses of the core were neglected.

Free vibration analysis of thick orthotropic plates was performed by Ghugal *et al.* (2011) using a trigonometric shear deformation theory. In their theory, the zero shear stress conditions on the top and bottom surfaces of the plates were satisfied. Rahmani *et al.* (2012) studied the free vibration and buckling analyses of circular cylindrical composite sandwich shells subjected to external loads based on the Love–Kirchhoff assumptions for the face sheets. In their theory, the in-plane stresses of the core and the out of stresses of the face sheets were neglected. Mochida *et al.* (2012) studied free vibration response of doubly curved shallow shells using approximate Galerkin method. Classical theory of elasticity and von-Karman's non-linear deformation theory were used by Rafieipour et al. (2013) to investigate free vibration analyses of laminated composite plates.

Using developed four-node quadrilateral element and the zigzag theory, Yasin and Kapuria (2013) studied the static and free vibration analysis of singly- and doubly-curved composite and sandwich shallow shells. In their theory, the transverse normal stresses were neglected. Ghavanloo and Fazelzadeh (2013) examined free vibration analysis of simply supported doubly curved shallow shells. Their formulation was based on Novozhilov's linear shallow shell theory. Using Donell's non-linear shallow shell theory and Kirchhoff's hypothesis, Awrejcewicz *et al.* (2013) studied free vibration analysis of doubly curved orthotropic shallow shells. Viola *et al.* (2013) used a 2D higher order shear deformation theory with nine parameters in order to analyze free vibration analysis of the thick laminated doubly curved shells and panels. Their main assumptions were based on small deflections and negligible normal stress and strain. A high-order model for the analysis of circular cylindrical composite sandwich shells subjected to low-velocity impact loads was presented by Khalili *et al.* (2014). In their theory, the impact behavior of the cylindrical composite sandwich shells was described by a high-order sandwich shell theory. Malekzadeh *et al.* (2014) applied the first-order shear deformation theory to study effects of some geometrical, physical and material parameters on response of the composite plates embedded with shape memory alloy (SMA) wires.

This study investigated free vibration analysis of double curved thick composite sandwich panels using a new improved higher order double curved sandwich panel theory and the second computational model of Frostig (2004). In this work, analytical solution of the displacement field of the core was presented in terms of the polynomials with unknown coefficients according to the second computational model of Frostig (2004). Furthermore, the formulation included accurate stress-resultant equations for composite sandwich structures, in which the terms $(1 + z_c / R_{xc})$ and $(1 + z_c / R_{yc})$ were imported in equations and exactly integrated. These coefficients could be very important in the structural analysis of thick double curved composite sandwich structures. Simply supported and fully clamped boundary conditions were considered. In order to assure accuracy of the present formulations, convergence of the results was examined in details.

2 THEORETICAL FORMULATION

2.1 Basic Assumptions

Consider a double curved thick composite sandwich panel which is composed of two composite laminated face sheets and a flexible core layer. Thickness of the top face sheet, bottom face sheet and core is h_t, h_b and h_c, respectively. The sandwich panel is supposed to have length a, width b and total thickness h, as shown in Figure 1. Orthogonal curvilinear coordinates $(x_i, y_i, z_i,\ i = t, b, c)$ are also shown in Figure 1 where t and b refer to the top and bottom face sheets of the panel, respectively. Curvature radii of the top face sheet, bottom face sheet and core in x-z and y-z planes are R_{tx}, R_{bx}, R_{cx} and R_{ty}, R_{by}, R_{cy}, respectively. The assumptions used in the present analysis were based on small deformations of linearly elastic materials.

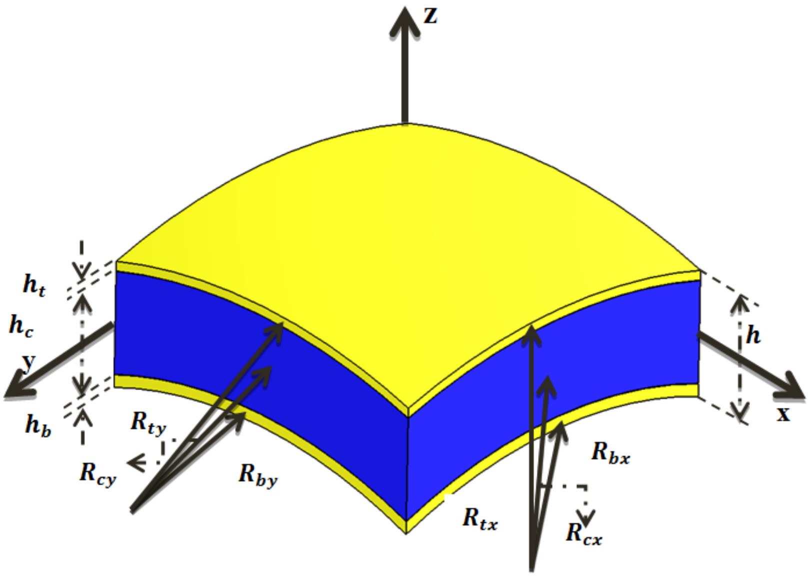

Figure 1: A double curved sandwich panel with laminated face sheets and orthogonal curvilinear coordinates.

2.2 Mathematical Formulation

Mathematical formulation consists of deriving the governing field equations of motion along appropriate boundary conditions of the face sheets and core. They are derived using the Hamilton's principle (Frostig 2004).

Using the first shear deformation theory, displacements u, v and w of the face sheets along the x, y (longitudinal) and z (thickness) axes are expressed through the following relations (Reddy 2003):

$$\begin{aligned} u_i(x,z,y,t) &= u_0^i(x,y,t) + z_i\psi_x^i(x,y,t) \\ v_i(x,z,y,t) &= v_0^i(x,y,t) + z_i\psi_y^i(x,y,t) \qquad ; \qquad (i{=}t,b) \\ w_i(x,z,y,t) &= w_0^i(x,y,t) \end{aligned} \tag{1}$$

where z_i is vertical coordinate of the each face sheet (i = t, b), measured upward from the mid-plane of each face sheet. Kinematic equations of the face sheets are as follows:

$$\begin{aligned} &\varepsilon_{xx}^i = \varepsilon_{0xx}^i + z_i\kappa_{xx}^i, \varepsilon_{yy}^i = \varepsilon_{0yy}^i + z_i\kappa_{yy}^i \varepsilon_{zz}^i = 0, \gamma_{xy}^i = 2\varepsilon_{xy}^i = \varepsilon_{0xy}^i + z_i\kappa_{xy}^i, \\ &\gamma_{xz}^i = 2\varepsilon_{xz}^i = \varepsilon_{0xz}^i, \gamma_{yz}^i = 2\varepsilon_{yz}^i = \varepsilon_{0yz}^i \qquad ; \qquad \left(i = t,b \right) \end{aligned} \tag{2}$$

where:

$$\varepsilon^i_{0xx}=\frac{\partial u^i_0}{\partial x}+\frac{w^i_0}{R_{xi}},\quad \varepsilon^i_{0yy}=\frac{\partial v^i_0}{\partial y}+\frac{w^i_0}{R_{yi}},$$
$$\varepsilon^i_{0xy}=\frac{\partial v^i_0}{\partial x}+\frac{\partial u^i_0}{\partial y},\ \varepsilon^i_{0xz}=\frac{\partial w^i_0}{\partial x}+\psi^i_x-\frac{u^i_0}{R_{xi}},\ \varepsilon^i_{0yz}=\frac{\partial w^i_0}{\partial y}+\psi^i_y-\frac{v^i_0}{R_{yi}} \tag{3}$$
$$\kappa^i_{xx}=\frac{\partial \psi^i_x}{\partial x},\qquad \kappa^i_{yy}=\frac{\partial \psi^i_y}{\partial y},\qquad \kappa^i_{xy}=\frac{\partial \psi^i_y}{\partial x}+\frac{\partial \psi^i_x}{\partial y}$$

For the thick core layer, displacement fields are based on the second Frostig's model (2004) as follows:

$$u_c\left(x,y,z,t\right)=(1+\frac{z}{R_{xc}})u^c_0\left(x,y,t\right)+z_c u^c_1\left(x,y,t\right)+z_c^2u^c_2\left(x,y,t\right)+z_c^3u^c_3\left(x,y,t\right),$$
$$v_c\left(x,y,z,t\right)=(1+\frac{z}{R_{yc}})v^c_0\left(x,y,t\right)+z_c v^c_1\left(x,y,t\right)+z_c^2v^c_2\left(x,y,t\right)+z_c^3\,v^c_3\left(x,y,t\right), \tag{4}$$
$$w_c\left(x,y,z,t\right)=w^c_0\left(x,y,t\right)+z_c w^c_1\left(x,y,t\right)+z_c^2w^c_2\left(x,y,t\right).$$

Based on small deformations, kinematic relations of the core layer are as follows:

$$\varepsilon^c_{xx}=\frac{1}{(1+z/R_{xc})}\left(\frac{\partial u_c}{\partial x}+\frac{w_c}{R_{xc}}\right)$$
$$\varepsilon^c_{yy}=\frac{1}{(1+z/R_{yc})}\left(\frac{\partial v_c}{\partial y}+\frac{w_c}{R_{yc}}\right)$$
$$\gamma^c_{xy}=2\,\varepsilon^c_{xy}=\frac{1}{(1+z/R_{xc})}\frac{\partial v_c}{\partial x}+\frac{1}{(1+z/R_{yc})}\frac{\partial u_c}{\partial y} \tag{5}$$
$$\gamma^c_{xz}=2\varepsilon^c_{xz}=\frac{1}{(1+z/R_{xc})}\left(\frac{\partial w_c}{\partial x}-\frac{u_c}{R_{xc}}\right)+\frac{\partial u_c}{\partial z}$$
$$\gamma^c_{yz}=2\varepsilon^c_{yz}=\frac{1}{(1+z/R_{yc})}\left(\frac{\partial w_c}{\partial y}-\frac{v_c}{R_{yc}}\right)+\frac{\partial v_c}{\partial z}$$

Assuming perfect bonding between the top and bottom face sheet–core interfaces, compatibility conditions are as shown below:

$$\begin{cases} u_c\left(z=z_{ci}\right)=u^i_0+\frac{1}{2}(-1)^k\ h_i\psi^i_x \\ v_c\left(z=z_{ci}\right)=v^i_0+\frac{1}{2}(-1)^k\ h_i\psi^i_y \\ w_c\left(z=z_{ci}\right)=w^i_0 \end{cases}\qquad \begin{cases} For\ \ i=t\rightarrow\left(k=1\,;\,z_{ct}=\frac{h_c}{2}\right) \\ For\ \ i=b\rightarrow\left(k=0\,;\,z_{cb}=-\frac{h_c}{2}\right)\end{cases} \tag{6}$$

Using Equations (4) and (6) and some simplifications, compatibility conditions can be written as follows:

$$
\begin{aligned}
u_2^c &= \frac{2(u_0^t + u_0^b) - h_t\psi_x^t + h_b\psi_x^b - 4u_0^c}{h_c^2}, u_3^c = \frac{4(u_0^t - u_0^b) - 2(h_t\psi_x^t + h_b\psi_x^b) - 4h_c u_1^c - \dfrac{4h_c u_0^c}{R_{xc}}}{h_c^3}, \\
v_2^c &= \frac{2(v_0^t + v_0^b) - h_t\psi_y^t + h_b\psi_y^b - 4v_0^c}{h_c^2}, v_3^c = \frac{4(v_0^t - v_0^b) - 2(h_t\psi_y^t + h_b\psi_y^b) - 4h_c v_1^c - \dfrac{4h_c v_0^c}{R_{yc}}}{h_c^3}, \\
w_1^c &= \frac{(w_0^t - w_0^b)}{h_c}, w_2^c = \frac{2(w_0^t + w_0^b) - 4w_0^c}{h_c^2}.
\end{aligned}
\tag{7}
$$

It can be seen in Equation (7) that the number of unknowns in the core layer is reduced to five. These unknowns are $u_0^c, u_1^c, v_0^c, v_1^c$ and w_0^c. Therefore, generally, all unknowns for a double curved composite sandwich panel are fifteen as follows:

$$
\left\{u_0^t, v_0^t, w_0^t, \psi_x^t, \psi_y^t, u_0^b, v_0^b, w_0^b, \psi_x^b, \psi_y^b, u_0^c, u_1^c, v_0^c, v_1^c, w_0^c\right\}
$$

The governing equations are derived using the Hamilton's principle which requires that:

$$
\int_0^t \delta L dt = \int_0^t [\delta K - \delta U] dt = 0 \tag{8}
$$

where δK and δU denote variation of kinetic energy and strain energy, respectively. Also, t is time duration between times t_1 and t_2, and δ denotes variation operator.

The first variation of kinetic energy (assuming homogeneous conditions for displacement and velocity with respect to time coordinate) can be written as follows:

$$
\delta K = -\sum_{i=t,b,c} \left[\iint_{A_i} \int_{-\frac{h_i}{2}}^{\frac{h_i}{2}} \rho_i \;\; \ddot{u}_i \delta u_i + \ddot{v}_i \delta v_i + \ddot{w}_i \delta w_i \;\; dz_i \, dA_i \right]; \qquad (i = t, b, c) \tag{9}
$$

where

$$
dA_c = (1 + \frac{z_c}{R_{xc}})(1 + \frac{z_c}{R_{yc}}) dx_c dy_c, \quad dA_i = dx_i dy_i, \quad (i = t, b)
$$

and ($\ddot{\circ}\dot{\circ}\dot{\circ}$ $\dot{\circ}\dot{\circ}\dot{\circ}$) denotes the second derivative in time. The first variation of internal potential energy of the sandwich panel is as follows:

$$
\begin{aligned}
\delta U = &\sum_{i=t,b} \left(\int_{V_i} \left(\sigma_{xx}^i \delta\varepsilon_{xx}^i + \sigma_{yy}^i \delta\varepsilon_{yy}^i + \tau_{xy}^i \delta\gamma_{xy}^i + \tau_{xz}^t \delta\gamma_{xz}^i + \tau_{yz}^i \delta\gamma_{yz}^i \right) dV_i \right) \\
&+ \int_{V_c} \left(\sigma_{xx}^c \delta\varepsilon_{xx}^c + \sigma_{yy}^c \delta\varepsilon_{yy}^c + \sigma_{zz}^c \delta\varepsilon_{zz}^c + \tau_{xy}^c \delta\gamma_{xy}^c + \tau_{xz}^c \delta\gamma_{xz}^c + \tau_{yz}^c \delta\gamma_{yz}^c \right) dV_c
\end{aligned}
\tag{10}
$$

where:

$$dV_c = dA_c dz_c = (1+\frac{z_c}{R_{xc}})(1+\frac{z_c}{R_{yc}})dx_c dy_c dz_c, dV_i = dA_i dz_i = dx_i dy_i dz_i \ ; \ (i=t,b)$$

Using the Hamilton's principle (Equations (8)-(10)) and the kinematic relations (Equations (1)-(7)), equations of motion are obtained as follows:

$$\begin{aligned}&\frac{Q_{xz}^t}{R_{tx}}+\frac{2}{h_c^2}M_{2xx,x}^c+\frac{4}{h_c^3}M_{3xx,x}^c+\frac{2}{h_c^2}M_{2yx,y}^c+\frac{4}{h_c^3}M_{3yx,y}^c+\frac{2}{R_{tx}h_c^2}M_{2xz}^c+\frac{4}{R_{tx}h_c^3}M_{3xz}^c-\\&\frac{4}{h_c^2}M_{1xz}^{*c}-\frac{12}{h_c^3}M_{2xz}^{*c}=\left(I_0^t+\frac{4I_4^c}{h_c^4}+\frac{16I_5^c}{h_c^5}+\frac{16I_6^c}{h_c^6}\right)\ddot{u}_0^t+\left(\frac{4I_4^c}{h_c^4}-\frac{16I_6^c}{h_c^6}\right)\ddot{u}_0^b+\\&\left(\frac{2}{h_c^2}(I_2^c+\frac{I_3^c}{R_{xc}})+\frac{4}{h_c^3}(I_3^c+\frac{I_4^c}{R_{xc}})-\frac{8I_4^c}{h_c^4}-\frac{8I_5^c}{h_c^4R_{xc}}-\frac{16I_5^c}{h_c^5}-\frac{16I_6^c}{R_{xc}h_c^5}\right)\ddot{u}_0^c+\\&\left(\frac{2I_3^c}{h_c^2}+\frac{4I_4^c}{h_c^3}-\frac{8I_5^c}{h_c^4}-\frac{16I_6^c}{h_c^5}\right)\ddot{u}_1^c+\left(I_1^t-\frac{2h_tI_4^c}{h_c^4}-\frac{8h_tI_5^c}{h_c^5}-\frac{8h_tI_6^c}{h_c^6}\right)\ddot{\psi}_x^t+\left(\frac{2h_bI_4^c}{h_c^4}-\frac{8h_bI_6^c}{h_c^6}\right)\ddot{\psi}_x^b\end{aligned} \quad (11)$$

$$\begin{aligned}&\frac{Q_{xz}^b}{R_{bx}}+\frac{2}{h_c^2}M_{2xx,x}^c-\frac{4}{h_c^3}M_{3xx,x}^c+\frac{2}{h_c^2}M_{2yx,y}^c-\frac{4}{h_c^3}M_{3yx,y}^c+\frac{2}{R_{bx}h_c^2}M_{2xz}^c-\frac{4}{R_{bx}h_c^3}M_{3xz}^c\\&-\frac{4}{h_c^2}M_{1xz}^{*c}+\frac{12}{h_c^3}M_{2xz}^{*c}=\left(\frac{4I_4^c}{h_c^4}-\frac{16I_6^c}{h_c^6}\right)\ddot{u}_0^t+\left(I_0^b+\frac{4I_4^c}{h_c^4}-\frac{16I_5^c}{h_c^5}+\frac{16I_6^c}{h_c^6}\right)\ddot{u}_0^b+\\&\left(\frac{2}{h_c^2}(I_2^c+\frac{I_3^c}{R_{xc}})-\frac{4}{h_c^3}(I_3^c+\frac{I_4^c}{R_{xc}})-\frac{8I_4^c}{h_c^4}-\frac{8I_5^c}{h_c^4R_{xc}}+\frac{16I_5^c}{h_c^5}+\frac{16I_6^c}{R_{xc}h_c^5}\right)\ddot{u}_0^c+\\&\left(\frac{2I_3^c}{h_c^2}-\frac{4I_4^c}{h_c^3}-\frac{8I_5^c}{h_c^4}+\frac{16I_6^c}{h_c^5}\right)\ddot{u}_1^c+\left(-\frac{2h_tI_4^c}{h_c^4}+\frac{8h_tI_6^c}{h_c^6}\right)\ddot{\psi}_x^t+\left(I_1^b+\frac{2h_bI_4^c}{h_c^4}-\frac{8h_bI_5^c}{h_c^5}+\frac{8h_bI_6^c}{h_c^6}\right)\ddot{\psi}_x^b\end{aligned} \quad (12)$$

$$\begin{aligned}&\frac{Q_{yz}^t}{R_{ty}}+\frac{2}{h_c^2}M_{2yy,y}^c+\frac{4}{h_c^3}M_{3yy,y}^c+\frac{2}{h_c^2}M_{2xy,x}^c+\frac{4}{h_c^3}M_{3xy,x}^c+\frac{2}{R_{cy}h_c^2}M_{2yz}^c+\frac{4}{R_{cy}h_c^3}M_{3yz}^c-\frac{4}{h_c^2}M_{1yz}^{*c}\\&-\frac{12}{h_c^3}M_{2yz}^{*c}=\left(I_0^t+\frac{4I_4^c}{h_c^4}+\frac{16I_5^c}{h_c^5}+\frac{16I_6^c}{h_c^6}\right)\ddot{v}_0^t+\left(\frac{4I_4^c}{h_c^4}-\frac{16I_6^c}{h_c^6}\right)\ddot{v}_0^b+\\&\left(\frac{2}{h_c^2}(I_2^c+\frac{I_3^c}{R_{yc}})+\frac{4}{h_c^3}(I_3^c+\frac{I_4^c}{R_{yc}})-\frac{8I_4^c}{h_c^4}-\frac{8I_5^c}{h_c^4R_{yc}}-\frac{16I_5^c}{h_c^5}-\frac{16I_6^c}{R_{yc}h_c^5}\right)\ddot{v}_0^c+\\&\left(\frac{2I_3^c}{h_c^2}+\frac{4I_4^c}{h_c^3}-\frac{8I_5^c}{h_c^4}-\frac{16I_6^c}{h_c^5}\right)\ddot{v}_1^c+\left(I_1^t-\frac{2h_tI_4^c}{h_c^4}-\frac{8h_tI_5^c}{h_c^5}-\frac{8h_tI_6^c}{h_c^6}\right)\ddot{\psi}_y^t+\left(\frac{2h_bI_4^c}{h_c^4}-\frac{8h_bI_6^c}{h_c^6}\right)\ddot{\psi}_y^b\end{aligned} \quad (13)$$

$$\frac{Q^b_{yz}}{R_{by}}+\frac{2}{h_c^2}M^c_{2yy,y}-\frac{4}{h_c^3}M^c_{3yy,y}+\frac{2}{h_c^2}M^c_{2xy,x}-\frac{4}{h_c^3}M^c_{3xy,x}+\frac{2}{R_{cy}h_c^2}M^c_{2yz}-\frac{4}{R_{cy}h_c^3}M^c_{3yz}$$
$$-\frac{4}{h_c^2}M^{*c}_{1yz}+\frac{12}{h_c^3}M^{*c}_{2yz}=\left(\frac{4I_4^c}{h_c^4}-\frac{16I_6^c}{h_c^6}\right)\ddot{v}_0^t+\left(I_0^b+\frac{4I_4^c}{h_c^4}-\frac{16I_5^c}{h_c^5}+\frac{16I_6^c}{h_c^6}\right)\ddot{v}_0^b+$$
$$\left(\frac{2}{h_c^2}(I_2^c+\frac{I_3^c}{R_{yc}})-\frac{4}{h_c^3}(I_3^c+\frac{I_4^c}{R_{yc}})-\frac{8I_4^c}{h_c^4}-\frac{8I_5^c}{h_c^4R_{yc}}+\frac{16I_5^c}{h_c^5}+\frac{16I_6^c}{R_{yc}h_c^5}\right)\ddot{v}_0^c+ \tag{14}$$
$$\left(\frac{2I_3^c}{h_c^2}-\frac{4I_4^c}{h_c^3}-\frac{8I_5^c}{h_c^4}+\frac{16I_6^c}{h_c^5}\right)\ddot{v}_1^c+\left(-\frac{2h_tI_4^c}{h_c^4}+\frac{8h_tI_6^c}{h_c^6}\right)\ddot{\psi}_y^t+\left(I_1^b+\frac{2h_bI_4^c}{h_c^4}-\frac{8h_bI_5^c}{h_c^5}+\frac{8h_bI_6^c}{h_c^6}\right)\ddot{\psi}_y^b$$

$$Q^t_{xz,x}+Q^t_{yz,y}-(\frac{N^t_{xx}}{R_{tx}}+\frac{N^t_{yy}}{R_{ty}})-\frac{R_z^c}{h_c}-\frac{1}{R_{cx}h_c}M^c_{1xx}-\frac{4}{h_c^2}M^c_z-\frac{2}{R_{cx}h_c^2}M^c_{2xx}-\frac{1}{R_{cy}h_c}M^c_{1yy}$$
$$-\frac{2}{R_{cy}h_c^2}M^c_{2yy}+\frac{1}{h_c}M^c_{1xz,x}+\frac{2}{h_c^2}M^c_{2xz,x}+\frac{1}{h_c}M^c_{1yz,y}+\frac{2}{h_c^2}M^c_{2yz,y} \tag{15}$$
$$=\left(I_0^t+\frac{I_2^c}{h_c^2}+\frac{4I_3^c}{h_c^3}+\frac{4I_4^c}{h_c^4}\right)\ddot{w}_0^t+\left(-\frac{I_2^c}{h_c^2}+\frac{4I_4^c}{h_c^4}\right)\ddot{w}_0^b+\left(\frac{I_1^c}{h_c}+\frac{2I_2^c}{h_c^2}-\frac{4I_3^c}{h_c^3}-\frac{8I_4^c}{h_c^4}\right)\ddot{w}_0^c$$

$$Q^b_{xz,x}+Q^b_{yz,y}-(\frac{N^b_{xx}}{R_{bx}}+\frac{N^b_{yy}}{R_{by}})+\frac{R_z^c}{h_c}+\frac{1}{R_{cx}h_c}M^c_{1xx}-\frac{4}{h_c^2}M^c_z-\frac{2}{R_{cx}h_c^2}M^c_{2xx}+\frac{1}{R_{cy}h_c}M^c_{1yy}-$$
$$\frac{2}{R_{cy}h_c^2}M^c_{2yy}-\frac{1}{h_c}M^c_{1xz,x}+\frac{2}{h_c^2}M^c_{2xz,x}-\frac{1}{h_c}M^c_{1yz,y}+\frac{2}{h_c^2}M^c_{2yz,y}=\left(-\frac{I_2^c}{h_c^2}+\frac{4I_4^c}{h_c^4}\right)\ddot{w}_0^t+ \tag{16}$$
$$\left(I_0^b+\frac{I_2^c}{h_c^2}-\frac{4I_3^c}{h_c^3}+\frac{4I_4^c}{h_c^4}\right)\ddot{w}_0^b+\left(-\frac{I_1^c}{h_c}+\frac{2I_2^c}{h_c^2}+\frac{4I_3^c}{h_c^3}-\frac{8I_4^c}{h_c^4}\right)\ddot{w}_0^c$$

$$M^t_{xx,x}+M^t_{xy,y}-Q^t_{xz}-\frac{h_t}{h_c^2}M^c_{2xx,x}-\frac{2h_t}{h_c^3}M^c_{3xx,x}-\frac{h_t}{h_c^2}M^c_{2yx,y}-\frac{2h_t}{h_c^3}M^c_{3yx,y}-\frac{h_t}{R_{cx}h_c^2}M^c_{2xz}$$
$$-\frac{2h_t}{R_{cx}h_c^2}M^c_{3xz}+\frac{2h_t}{h_c^2}M^{*c}_{1xz}+\frac{6h_t}{h_c^3}M^{*c}_{2xz}=\left(I_1^t-\frac{2h_tI_4^c}{h_c^4}+\frac{8h_tI_5^c}{h_c^5}-\frac{8h_tI_6^c}{h_c^6}\right)\ddot{u}_0^t+(-\frac{2h_tI_4^c}{h_c^4}+\frac{8h_tI_6^c}{h_c^6})\ddot{u}_0^b$$
$$+\left(-\frac{h_t}{h_c^2}(I_2^c+\frac{I_3^c}{R_{xc}})-\frac{2h_t}{h_c^3}(I_3^c+\frac{I_4^c}{R_{xc}})+\frac{4h_tI_4^c}{h_c^4}+\frac{4h_tI_5^c}{R_{xc}h_c^4}+\frac{8h_tI_5^c}{h_c^5}+\frac{8h_tI_6^c}{R_{xc}h_c^5}\right)\ddot{u}_0^c+ \tag{17}$$
$$\left(-\frac{h_tI_3^c}{h_c^2}-\frac{2h_tI_4^c}{h_c^3}+\frac{4h_tI_5^c}{h_c^4}+\frac{8h_tI_6^c}{h_c^5}\right)\ddot{u}_1^c+\left(-\frac{h_th_bI_4^c}{h_c^4}+\frac{4h_th_bI_6^c}{h_c^6}\right)\ddot{\psi}_x^b+\left(I_2^t+\frac{h_t^2I_4^c}{h_c^4}+\frac{4h_t^2I_5^c}{h_c^5}+\frac{4h_t^2I_6^c}{h_c^6}\right)\ddot{\psi}_x^t$$

$$
\begin{aligned}
&M^{b}_{xx,x}+M^{b}_{xy,y}-Q^{b}_{xz}+\frac{h_b}{h_c^2}M^{c}_{2xx,x}-\frac{2h_b}{h_c^3}M^{c}_{3xx,x}+\frac{h_b}{h_c^2}M^{c}_{2yx,y}-\frac{2h_b}{h_c^3}M^{c}_{3yx,y}+\frac{h_b}{R_{cx}h_c^2}M^{c}_{2xz}-\\
&\frac{2h_b}{R_{cx}h_c^2}M^{c}_{3xz}-\frac{2h_b}{h_c^2}M^{*c}_{1xz}+\frac{6h_b}{h_c^3}M^{*c}_{2xz}=\left(\frac{2h_tI_4^c}{h_c^4}-\frac{8h_tI_6^c}{h_c^6}\right)\ddot{u}_0^t+(I_1^b+\frac{2h_bI_4^c}{h_c^4}-\frac{8h_bI_5^c}{h_c^5}+\frac{8h_bI_6^c}{h_c^6})\ddot{u}_0^b+\\
&\left(\frac{h_b}{h_c^2}(I_2^c+\frac{I_3^c}{R_{xc}})-\frac{2h_b}{h_c^3}(I_3^c+\frac{I_4^c}{R_{xc}})-\frac{4h_bI_4^c}{h_c^4}-\frac{4h_bI_5^c}{R_{xc}h_c^4}+\frac{8h_bI_5^c}{h_c^5}+\frac{8h_bI_6^c}{R_{xc}h_c^5}\right)\ddot{u}_0^c+\\
&\left(\frac{h_bI_3^c}{h_c^2}-\frac{2h_bI_4^c}{h_c^3}-\frac{4h_bI_5^c}{h_c^4}+\frac{8h_bI_6^c}{h_c^5}\right)\ddot{u}_1^c+\left(-\frac{h_th_bI_4^c}{h_c^4}+\frac{4h_th_bI_6^c}{h_c^6}\right)\ddot{\psi}_x^t+\left(I_2^b+\frac{h_b^2I_4^c}{h_c^4}-\frac{4h_b^2I_5^c}{h_c^5}+\frac{4h_b^2I_6^c}{h_c^6}\right)\ddot{\psi}_x^b
\end{aligned}
\tag{18}
$$

$$
\begin{aligned}
&M^{t}_{xy,x}+M^{t}_{yy,y}-Q^{t}_{yz}-\frac{h_t}{h_c^2}M^{c}_{2yy,y}-\frac{2h_t}{h_c^3}M^{c}_{3yy,y}-\frac{h_t}{h_c^2}M^{c}_{2xy,x}-\frac{2h_t}{h_c^3}M^{c}_{3xy,x}-\frac{h_t}{R_{cx}h_c^2}M^{c}_{2yz}-\\
&\frac{2h_t}{R_{cx}h_c^2}M^{c}_{3yz}+\frac{2h_t}{h_c^2}M^{*c}_{1yz}+\frac{6h_t}{h_c^3}M^{*c}_{2yz}=\left(I_1^t-\frac{2h_tI_4^c}{h_c^4}+\frac{8h_tI_5^c}{h_c^5}-\frac{8h_tI_6^c}{h_c^6}\right)\ddot{v}_0^t+\left(-\frac{2h_tI_4^c}{h_c^4}+\frac{8h_tI_6^c}{h_c^6}\right)\ddot{v}_0^b+\\
&\left(-\frac{h_t}{h_c^2}(I_2^c+\frac{I_3^c}{R_{yc}})-\frac{2h_t}{h_c^3}(I_3^c+\frac{I_4^c}{R_{yc}})+\frac{4h_tI_4^c}{h_c^4}+\frac{4h_tI_5^c}{R_{yc}h_c^4}+\frac{8h_tI_5^c}{h_c^5}+\frac{8h_tI_6^c}{R_{yc}h_c^5}\right)\ddot{v}_0^c+\\
&\left(-\frac{h_tI_3^c}{h_c^2}-\frac{2h_tI_4^c}{h_c^3}+\frac{4h_tI_5^c}{h_c^4}+\frac{8h_tI_6^c}{h_c^5}\right)\ddot{v}_1^c+\left(I_2^t+\frac{h_t^2I_4^c}{h_c^4}+\frac{4h_t^2I_5^c}{h_c^5}+\frac{4h_t^2I_6^c}{h_c^6}\right)\ddot{\psi}_y^t+\left(-\frac{h_th_bI_4^c}{h_c^4}+\frac{4h_th_bI_6^c}{h_c^6}\right)\ddot{\psi}_y^b
\end{aligned}
\tag{19}
$$

$$
\begin{aligned}
&M^{b}_{xy,x}+M^{b}_{yy,y}-Q^{b}_{yz}+\frac{h_b}{h_c^2}M^{c}_{2yy,y}-\frac{2h_b}{h_c^3}M^{c}_{3yy,y}+\frac{h_b}{h_c^2}M^{c}_{2xy,x}-\frac{2h_b}{h_c^3}M^{c}_{3xy,x}+\frac{h_b}{R_{cy}h_c^2}M^{c}_{2yz}-\frac{2h_b}{R_{cy}h_c^2}M^{c}_{3yz}\\
&-\frac{2h_b}{h_c^2}M^{*c}_{1yz}+\frac{6h_b}{h_c^3}M^{*c}_{2yz}=\left(\frac{2h_tI_4^c}{h_c^4}-\frac{8h_tI_6^c}{h_c^6}\right)\ddot{v}_0^t+\left(I_1^b+\frac{2h_bI_4^c}{h_c^4}-\frac{8h_bI_5^c}{h_c^5}+\frac{8h_bI_6^c}{h_c^6}\right)\ddot{v}_0^b+\\
&\left(\frac{h_b}{h_c^2}(I_2^c+\frac{I_3^c}{R_{yc}})-\frac{2h_b}{h_c^3}(I_3^c+\frac{I_4^c}{R_{yc}})-\frac{4h_bI_4^c}{h_c^4}-\frac{4h_bI_5^c}{R_{yc}h_c^4}+\frac{8h_bI_5^c}{h_c^5}+\frac{8h_bI_6^c}{R_{yc}h_c^5}\right)\ddot{v}_0^c+\\
&\left(\frac{h_bI_3^c}{h_c^2}-\frac{2h_bI_4^c}{h_c^3}-\frac{4h_bI_5^c}{h_c^4}+\frac{8h_bI_6^c}{h_c^5}\right)\ddot{v}_1^c+\left(-\frac{h_th_bI_4^c}{h_c^4}+\frac{4h_th_bI_6^c}{h_c^6}\right)\ddot{\psi}_y^t+\left(I_2^b+\frac{h_b^2I_4^c}{h_c^4}-\frac{4h_b^2I_5^c}{h_c^5}+\frac{4h_b^2I_6^c}{h_c^6}\right)\ddot{\psi}_y^b
\end{aligned}
\tag{20}
$$

$$(N^c_{xx,x}+N^c_{yx,y}-\frac{4}{h_c^2}M^c_{2xx,x}-\frac{4}{R_{cx}h_c^2}M^c_{3xx,x}+\frac{1}{R_{cx}}M^c_{1yx,y}-\frac{4}{h_c^2}M^c_{2yx,y}-\frac{4}{R_{cx}h_c^2}M^c_{3yx,y}+\frac{1}{R_{cx}}N^c_{xz}-$$
$$\frac{4}{R_{cx}h_c^2}M^c_{2xz}-\frac{4}{R_{cx}^2h_c^2}M^c_{3xz}+\frac{8}{h_c^2}M^{*c}_{1xz}+\frac{12}{R_{cx}h_c^2}M^{*c}_{2xz}-\frac{1}{R_{cx}}N^{*c}_{xz})=\Bigg(I^c_0+\frac{I^c_2}{R^2_{xc}}+\frac{2I^c_1}{R_{xc}}-\frac{8}{h_c^2}(I^c_2+\frac{I^c_3}{R_{xc}})$$
$$-\frac{8}{h_c^2R_{xc}}(I^c_3+\frac{I^c_4}{R_{xc}})+\frac{16I^c_4}{h_c^4}+\frac{32I^c_5}{R_{xc}h_c^4}+\frac{16I^c_6}{R^2_{xc}h_c^4}\Bigg)\ddot{u}^c_0+\Bigg(I^c_1+\frac{I^c_2}{R_{xc}}-\frac{8I^c_3}{h_c^2}-\frac{8I^c_4}{h_c^2R_{xc}}+\frac{16I^c_5}{h_c^4}+\frac{16I^c_6}{R_{xc}h_c^4}\Bigg)\ddot{u}^c_1$$
$$+\Bigg(\frac{2}{h_c^2}(I^c_2+\frac{I^c_3}{R_{xc}})-\frac{4}{h_c^3}(I^c_3+\frac{I^c_4}{R_{xc}})-\frac{8I^c_4}{h_c^4}+\frac{16I^c_5}{h_c^5}-\frac{8I^c_5}{R_{xc}h_c^4}+\frac{16I^c_6}{R_{xc}h_c^5}\Bigg)\ddot{u}^b_0+(\frac{2}{h_c^2}(I^c_2+\frac{I^c_3}{R_{xc}})+\frac{4}{h_c^3}(I^c_3+\frac{I^c_4}{R_{xc}}) \tag{21}$$
$$-\frac{8I^c_4}{h_c^4}-\frac{16I^c_5}{h_c^5}-\frac{8I^c_5}{R_{xc}h_c^4}-\frac{16I^c_6}{R_{xc}h_c^5})\ddot{u}^t_0+\Bigg(\frac{h_b}{h_c^2}(I^c_2+\frac{I^c_3}{R_{xc}})-\frac{2h_b}{h_c^3}(I^c_3+\frac{I^c_4}{R_{xc}})-\frac{4h_bI^c_4}{h_c^4}+\frac{8h_bI^c_5}{h_c^5}-\frac{4h_ch_bI^c_5}{R_{xc}h_c^5}+$$
$$\frac{8h_ch_bI^c_6}{R_{xc}h_c^6}\Bigg)\ddot{\psi}^b_x+\Bigg(-\frac{h_t}{h_c^2}(I^c_2+\frac{I^c_3}{R_{xc}})-\frac{2h_t}{h_c^3}(I^c_3+\frac{I^c_4}{R_{xc}})+\frac{4h_tI^c_4}{h_c^4}+\frac{8h_tI^c_5}{h_c^5}+\frac{4h_ch_tI^c_5}{R_{xc}h_c^5}+\frac{8h_ch_tI^c_6}{R_{xc}h_c^6}\Bigg)\ddot{\psi}^t_x$$

$$M^c_{1xx,x}-N^{*c}_{xz}-\frac{4}{h_c^2}M^c_{3xx,x}+M^c_{1yx,y}-\frac{4}{h_c^2}M^c_{3yx,y}+\frac{1}{R_{cx}}M^c_{1xz}-\frac{4}{R_{cx}h_c^2}M^c_{3xz}+\frac{12}{h_c^2}M^{*c}_{2xz}=$$
$$\Bigg(\frac{2I^c_3}{h_c^2}+\frac{4I^c_4}{h_c^3}-\frac{8I^c_5}{h_c^4}-\frac{16I^c_6}{h_c^5}\Bigg)\ddot{u}^t_0+\Bigg(\frac{2I^c_3}{h_c^2}-\frac{4I^c_4}{h_c^3}-\frac{8I^c_5}{h_c^4}+\frac{16I^c_6}{h_c^5}\Bigg)\ddot{u}^b_0+$$
$$\Bigg(I^c_1+\frac{I^c_2}{R_{xc}}-\frac{8I^c_3}{h_c^2}-\frac{8I^c_4}{h_c^2R_{xc}}+\frac{16I^c_5}{h_c^4}+\frac{16I^c_6}{R_{xc}h_c^4}\Bigg)\ddot{u}^c_0+\Bigg(I^c_2-\frac{8I^c_4}{h_c^2}+\frac{16I^c_6}{h_c^4}\Bigg)\ddot{u}^c_1+ \tag{22}$$
$$\Bigg(-\frac{h_tI^c_3}{h_c^2}-\frac{2h_tI^c_4}{h_c^3}+\frac{4h_tI^c_5}{h_c^4}+\frac{8h_tI^c_6}{h_c^5}\Bigg)\ddot{\psi}^t_x+\Bigg(\frac{h_bI^c_3}{h_c^2}-\frac{2h_bI^c_4}{h_c^3}-\frac{4h_bI^c_5}{h_c^4}+\frac{8h_bI^c_6}{h_c^5}\Bigg)\ddot{\psi}^b_x$$

$$
\begin{aligned}
&N^c_{yy,y}+N^c_{xy,x}-\frac{4}{h_c^2}M^c_{2yy,y}-\frac{4}{R_{cy}h_c^2}M^c_{3yy,y}+\frac{1}{R_{cy}}M^c_{1xy,x}-\frac{4}{h_c^2}M^c_{2xy,x}-\frac{4}{R_{cy}h_c^2}M^c_{3xy,x}\\
&+\frac{1}{R_{cy}}N^c_{yz}-\frac{4}{R_{cy}h_c^2}M^c_{2yz}-\frac{4}{R_{cy}^2h_c^2}M^c_{3yz}+\frac{8}{h_c^2}M^{*c}_{1yz}+\frac{12}{R_{cy}h_c^2}M^{*c}_{2yz}-\frac{1}{R_{cy}}N^{*c}_{yz}=\\
&\left(\frac{2}{h_c^2}(I_2^c+\frac{I_3^c}{R_{yc}})+\frac{4}{h_c^3}(I_3^c+\frac{I_4^c}{R_{yc}})-\frac{8I_4^c}{h_c^4}-\frac{16I_5^c}{h_c^5}-\frac{8I_5^c}{R_{yc}h_c^4}-\frac{16I_6^c}{R_{yc}h_c^5}\right)\ddot{v}_0^t+\\
&\left(\frac{2}{h_c^2}(I_2^c+\frac{I_3^c}{R_{yc}})-\frac{4}{h_c^3}(I_3^c+\frac{I_4^c}{R_{yc}})-\frac{8I_4^c}{h_c^4}+\frac{16I_5^c}{h_c^5}-\frac{8I_5^c}{R_{yc}h_c^4}+\frac{16I_6^c}{R_{yc}h_c^5}\right)\ddot{v}_0^b+\\
&\left(I_0^c+\frac{I_2^c}{R_{yc}^2}+\frac{2I_1^c}{R_{yc}}-\frac{8}{h_c^2}(I_2^c+\frac{I_3^c}{R_{yc}})-\frac{8}{h_c^2R_{yc}}(I_3^c+\frac{I_4^c}{R_{yc}})+\frac{16I_4^c}{h_c^4}+\frac{32I_5^c}{R_{yc}h_c^4}+\frac{16I_6^c}{R_{yc}^2h_c^4}\right)\ddot{v}_0^c+\\
&\left(I_1^c+\frac{I_2^c}{R_{yc}}-\frac{8I_3^c}{h_c^2}-\frac{8I_4^c}{h_c^2R_{yc}}+\frac{16I_5^c}{h_c^4}+\frac{16I_6^c}{R_{yc}h_c^4}\right)\ddot{v}_1^c+\\
&\left(-\frac{h_t}{h_c^2}(I_2^c+\frac{I_3^c}{R_{yc}})-\frac{2h_t}{h_c^3}(I_3^c+\frac{I_4^c}{R_{yc}})+\frac{4h_tI_4^c}{h_c^4}+\frac{8h_tI_5^c}{h_c^5}+\frac{4h_ch_tI_5^c}{R_{yc}h_c^5}+\frac{8h_ch_tI_6^c}{R_{yc}h_c^6}\right)\ddot{\psi}_x^t+\\
&\left(\frac{h_b}{h_c^2}(I_2^c+\frac{I_3^c}{R_{yc}})-\frac{2h_b}{h_c^3}(I_3^c+\frac{I_4^c}{R_{yc}})-\frac{4h_bI_4^c}{h_c^4}+\frac{8h_bI_5^c}{h_c^5}-\frac{4h_ch_bI_5^c}{R_{yc}h_c^5}+\frac{8h_ch_bI_6^c}{R_{cy}h_c^6}\right)\ddot{\psi}_y^b
\end{aligned}
\tag{23}
$$

$$
\begin{aligned}
&M^c_{1yy,y}-N^{*c}_{yz}-\frac{4}{h_c^2}M^c_{3yy,y}+M^c_{1xy,x}-\frac{4}{h_c^2}M^c_{3xy,x}+\frac{1}{R_{cy}}M^c_{1yz}-\frac{4}{R_{cy}h_c^2}M^c_{3yz}+\\
&\frac{12}{h_c^2}M^{*c}_{2yz}=\left(\frac{2I_3^c}{h_c^2}+\frac{4I_4^c}{h_c^3}-\frac{8I_5^c}{h_c^4}-\frac{16I_6^c}{h_c^5}\right)\ddot{v}_0^t+\left(\frac{2I_3^c}{h_c^2}-\frac{4I_4^c}{h_c^3}-\frac{8I_5^c}{h_c^4}+\frac{16I_6^c}{h_c^5}\right)\ddot{v}_0^b+\\
&\left(I_1^c+\frac{I_2^c}{R_{yc}}-\frac{8I_3^c}{h_c^2}-\frac{8I_4^c}{h_c^2R_{yc}}+\frac{16I_5^c}{h_c^4}+\frac{16I_6^c}{R_{yc}h_c^4}\right)\ddot{v}_0^c+\left(I_2^c-\frac{8I_4^c}{h_c^2}+\frac{16I_6^c}{h_c^4}\right)\ddot{v}_1^c+\\
&\left(-\frac{h_tI_3^c}{h_c^2}-\frac{2h_tI_4^c}{h_c^3}+\frac{4h_tI_5^c}{h_c^4}+\frac{8h_tI_6^c}{h_c^5}\right)\ddot{\psi}_y^t+\left(\frac{h_bI_3^c}{h_c^2}-\frac{2h_bI_4^c}{h_c^3}-\frac{4h_bI_5^c}{h_c^4}+\frac{8h_bI_6^c}{h_c^5}\right)\ddot{\psi}_y^b
\end{aligned}
\tag{24}
$$

$$
\begin{aligned}
&N^c_{xz,x}+N^c_{yz,y}+\frac{8}{h_c^2}M^c_z-\frac{1}{R_{xc}}N^c_{xx}+\frac{4}{R_{xc}h_c^2}M^c_{2xx}-\frac{1}{R_{yc}}N^c_{yy}+\frac{4}{R_{yc}h_c^2}M^c_{2yy}-\frac{4}{h_c^2}M^c_{2xz,x}-\\
&\frac{4}{h_c^2}M^c_{2yz,y}=\left(\frac{I_1^c}{h_c}+\frac{2I_2^c}{h_c^2}-\frac{4I_3^c}{h_c^3}-\frac{8I_4^c}{h_c^4}\right)\ddot{w}_0^t+\left(-\frac{I_1^c}{h_c}+\frac{2I_2^c}{h_c^2}+\frac{4I_3^c}{h_c^3}-\frac{8I_4^c}{h_c^4}\right)\ddot{w}_0^b+\left(I_0^c-\frac{8I_2^c}{h_c^2}+\frac{16I_4^c}{h_c^4}\right)\ddot{w}_0^c
\end{aligned}
\tag{25}
$$

In Equations (11)-(25), $I_n^c\left(n=0,\ 1,\dots,6\right)$ are moments of inertia for the core layer, as indicated below:

$$
I_n^c=\int_{-\frac{h_c}{2}}^{\frac{h_c}{2}}\rho_c z_c^{\,n}(1+\frac{z_c}{R_{xc}})(1+\frac{z_c}{R_{yc}})dz_c\,;n=0,1,\dots,6 \tag{26}
$$

Stress resultants per unit length for the core layer are defined as demonstrated below:

$$\begin{Bmatrix} N_{xx}^{c} \\ N_{yy}^{c} \\ N_{xy}^{c} \\ N_{yx}^{c} \end{Bmatrix} = \int_{-h_c/2}^{h_c/2} \begin{Bmatrix} \sigma_{xx}^{c}(1+\frac{z_c}{R_{yc}}) \\ \sigma_{yy}^{c}(1+\frac{z_c}{R_{xc}}) \\ \sigma_{xy}^{c}(1+\frac{z_c}{R_{yc}}) \\ \sigma_{xy}^{c}(1+\frac{z_c}{R_{xc}}) \end{Bmatrix} dz_c, \begin{Bmatrix} M_{nxx}^{c} \\ M_{nyy}^{c} \\ M_{nxy}^{c} \\ M_{nyx}^{c} \end{Bmatrix} = \int_{-h_c/2}^{h_c/2} z_c^{n} \begin{Bmatrix} \sigma_{xx}^{c}(1+\frac{z_c}{R_{yc}}) \\ \sigma_{yy}^{c}(1+\frac{z_c}{R_{xc}}) \\ \sigma_{xy}^{c}(1+\frac{z_c}{R_{yc}}) \\ \sigma_{xy}^{c}(1+\frac{z_c}{R_{xc}}) \end{Bmatrix} dz_c, \begin{Bmatrix} N_{xz}^{c} \\ N_{yz}^{c} \\ M_{nxz}^{c} \\ M_{nyz}^{c} \end{Bmatrix} = \int_{-h_c/2}^{h_c/2} \begin{Bmatrix} \sigma_{xz}^{c}(1+\frac{z_c}{R_{yc}}) \\ \sigma_{yz}^{c}(1+\frac{z_c}{R_{xc}}) \\ z_c^{n}\sigma_{xz}^{c}(1+\frac{z_c}{R_{yc}}) \\ z_c^{n}\sigma_{yz}^{c}(1+\frac{z_c}{R_{xc}}) \end{Bmatrix} dz_c \tag{27}$$

$$\begin{Bmatrix} N_{xz}^{*c} \\ N_{yz}^{*c} \\ M_{nxz}^{*c} \\ M_{nyz}^{*c} \end{Bmatrix} = \int_{-h_c/2}^{h_c/2} \begin{Bmatrix} \sigma_{xz}^{c} \\ \sigma_{yz}^{c} \\ z_c^{n}\sigma_{xz}^{c} \\ z_c^{n}\sigma_{yz}^{c} \end{Bmatrix} (1+\frac{z_c}{R_{xc}})(1+\frac{z_c}{R_{yc}}) dz_c, \{R_z^c, M_z^c\} = \int_{-h_c/2}^{h_c/2} (1, z_c)\sigma_{zz}^{c}(1+\frac{z_c}{R_{xc}})(1+\frac{z_c}{R_{yc}}) dz_c.$$

Due to the radii of curvature are much larger than the thickness of the face sheets, in this paper 1+z/R for the face sheets can be approximated to 1. Therefore, stress resultants per unit length for the face sheets can be defined as follows:

$$\begin{Bmatrix} N_{xx}^{i} \\ N_{yy}^{i} \\ N_{xy}^{i} \\ N_{yx}^{i} \end{Bmatrix} = \int_{-h_i/2}^{h_i/2} \begin{Bmatrix} \sigma_{xx}^{i} \\ \sigma_{yy}^{i} \\ \sigma_{xy}^{i} \\ \sigma_{xy}^{i} \end{Bmatrix} dz_i, \begin{Bmatrix} M_{xx}^{i} \\ M_{yy}^{i} \\ M_{xy}^{i} \\ M_{yx}^{i} \end{Bmatrix} = \int_{-h_i/2}^{h_i/2} z_i \begin{Bmatrix} \sigma_{xx}^{i} \\ \sigma_{yy}^{i} \\ \sigma_{xy}^{i} \\ \sigma_{xy}^{i} \end{Bmatrix} dz_i, \begin{Bmatrix} Q_{xz}^{i} \\ Q_{yz}^{i} \end{Bmatrix} = k_s \int_{-h_i/2}^{h_i/2} \begin{Bmatrix} \sigma_{xz}^{i} \\ \sigma_{yz}^{i} \end{Bmatrix} dz_i \ ; i = t, b \tag{28}$$

Where k_s is the shear correction factor.

Constitutive equations for in-plane stress resultants based on the first order shear deformation laminate theory are defined as (Reddy, 2003):

$$\begin{aligned}
N_{xx}^{i} &= A_{11}^{i}u_{,x}^{i} + A_{12}^{i}v_{,y}^{i} + A_{16}^{i}(u_{,y}^{i} + v_{,x}^{i}) + B_{11}^{i}\psi_{x,x}^{i} + B_{12}^{i}\psi_{y,y}^{i} + B_{16}^{i}(\psi_{x,y}^{i} + \psi_{y,x}^{i}) \\
N_{yy}^{i} &= A_{12}^{i}u_{,x}^{i} + A_{22}^{i}v_{,y}^{i} + A_{26}^{i}(u_{,y}^{i} + v_{,x}^{i}) + B_{12}^{i}\psi_{x,x}^{i} + B_{22}^{i}\psi_{y,y}^{i} + B_{26}^{i}(\psi_{x,y}^{i} + \psi_{y,x}^{i}) \\
N_{xy}^{i} &= A_{16}^{i}u_{,x}^{i} + A_{26}^{i}v_{,y}^{i} + A_{66}^{i}(u_{,y}^{i} + v_{,x}^{i}) + B_{16}^{i}\psi_{x,x}^{i} + B_{26}^{i}\psi_{y,y}^{i} + B_{66}^{i}(\psi_{x,y}^{i} + \psi_{y,x}^{i}) \\
M_{xx}^{i} &= B_{11}^{i}u_{,x}^{i} + B_{12}^{i}v_{,y}^{i} + B_{16}^{i}(u_{,y}^{i} + v_{,x}^{i}) + D_{11}^{i}\psi_{x,x}^{i} + D_{12}^{i}\psi_{y,y}^{i} + D_{16}^{i}(\psi_{x,y}^{i} + \psi_{y,x}^{i}) \\
M_{yy}^{i} &= B_{12}^{i}u_{,x}^{i} + B_{22}^{i}v_{,y}^{i} + B_{26}^{i}(u_{,y}^{i} + v_{,x}^{i}) + D_{12}^{i}\psi_{x,x}^{i} + D_{22}^{i}\psi_{y,y}^{i} + D_{26}^{i}(\psi_{x,y}^{i} + \psi_{y,x}^{i}) \\
M_{xy}^{i} &= B_{16}^{i}u_{,x}^{i} + B_{26}^{i}v_{,y}^{i} + B_{66}^{i}(u_{,y}^{i} + v_{,x}^{i}) + D_{16}^{i}\psi_{x,x}^{i} + D_{26}^{i}\psi_{y,y}^{i} + B_{66}^{i}(\psi_{x,y}^{i} + \psi_{y,x}^{i}) \\
Q_{yz}^{i} &= k[A_{44}^{i}(\psi_{y}^{i} + w_{,y}^{i}) + A_{45}^{i}(\psi_{x}^{i} + w_{,x}^{i})] \\
Q_{xz}^{i} &= k[A_{45}^{i}(\psi_{y}^{i} + w_{,y}^{i}) + A_{55}^{i}(\psi_{x}^{i} + w_{,x}^{i})] \qquad i = (t,b)
\end{aligned} \tag{29}$$

where A_{ij} , B_{ij} and D_{ij} are extensional, bending-extensional coupling and bending stiffnesses, respectively.

3 ANALYTICAL SOLUTION

Displacement fields based on the double Fourier series for a double curved composite sandwich panel with simply supported boundary condition at the top and bottom face sheets are assumed to be in the following form ($j = t,b$):

$$\begin{bmatrix} u_0^j(x,y,t) \\ v_0^j(x,y,t) \\ w_0^j(x,y,t) \\ \psi_x^j(x,y,t) \\ \psi_y^j(x,y,t) \\ u_k^c(x,y,t) \\ v_k^c(x,y,t) \\ w_l^c(x,y,t) \end{bmatrix} = \sum_{n=1}^{\infty}\sum_{m=1}^{\infty} \begin{bmatrix} U_{0mn}^j \cos(\alpha_m x)\sin(\beta_n y) \\ V_{0mn}^j \sin(\alpha_m x)\cos(\beta_n y) \\ W_{0mn}^j \sin(\alpha_m x)\sin(\beta_n y) \\ \Psi_{xmn}^j \cos(\alpha_m x)\sin(\beta_n y) \\ \Psi_{ymn}^j \sin(\alpha_m x)\cos(\beta_n y) \\ U_{kmn}^c \cos(\alpha_m x)\sin(\beta_n y) \\ V_{kmn}^c \sin(\alpha_m x)\cos(\beta_n y) \\ W_{lmn}^c \sin(\alpha_m x)\sin(\beta_n y) \end{bmatrix} e^{i\omega t}, \ (k=0,1,2,3),\ (l=0,1,2) \tag{30}$$

where $\alpha_m = \dfrac{m\pi}{a}$ and $\beta_n = \dfrac{n\pi}{b}$.

When all edges are clamped, functions $\cos(\alpha_m x)$ and $\cos(\beta_n y)$ in the above series expansions must be replaced with $\sin(\alpha_m x)$ and $\sin(\alpha_m y)$, respectively.

In Equation (30), U_{0mn}^j , V_{0mn}^j , W_{0mn}^j , Ψ_{xmn}^j , Ψ_{ymn}^j , U_{kmn}^c , V_{kmn}^c and W_{lmn}^c are the Fourier coefficients and m and n are half wave numbers along x and y directions, respectively. By substituting stress resultants (Equation (27)), compatibility conditions (Equation (7)) and displacement field (Equation (30)) in the governing equations (Equations (11)-(25)), applying the Galerkin method and collecting coefficients, the eigenvalue equation is obtained as follows:

$$[K - \lambda_{mn} M]\{c\} = \{0\} \tag{31}$$

where

$$\{c\} = \{U_{0mn}^t, U_{0mn}^b, V_{0mn}^t, V_{0mn}^b, W_{0mn}^t, W_{0mn}^b, \psi_{xmn}^t, \psi_{xmn}^b, \psi_{ymn}^t, \psi_{ymn}^b, U_{0mn}^c, V_{0mn}^c, U_{1mn}^c, V_{1mn}^c, W_{0mn}^c\}^T$$

where $\lambda_{mn} = \omega_{mn}^2$ and {c} is displacement vector for all the values of m and n. Also [K] and [M] are stiffness and mass matrices, respectively. The above eigenvalue equation can be solved for various eigenvalues and associated eigenvectors.

4 VALIDATION OF THE RESULTS

In order to validate the present method and demonstrate its capability, the results obtained from the present theory were compared with recent theoretical and numerical results found in the literature. Also, the results were compared with those obtained from finite element ABAQUS software.

Example 1: Free vibration analysis of a flat composite sandwich panel with SSSS B.C.

In this example, a flat sandwich panel with laminated face sheets, PVC foam core and simply supported boundary conditions (SSSS) was considered. The lay-up sequences for face sheets were [0/90/0] and the sandwich panel was symmetric about the mid-plane. Mechanical properties of the face sheets and foam core are given in Table 1.

PVC foam core	Laminate face sheets
$E_1 = E_2 = E_3 = 0.10363$ GPa, $G_{12} = G_{13} = G_{23} = 0.05$ GPa, $\nu = 0.32$, $\rho = 130$ Kg / m^3.	$E_1 = 24.51$ GPa, $E_2 = E_3 = 7.77$ GPa, $G_{12} = G_{13} = 3.34$ GPa, $G_{23} = 1.34$GPa, $\nu_{12} = \nu_{13} = 0.078$, $\nu_{23} = 0.49$, $\rho = 1800$ Kg / m^3.

Table 1: Material properties of the composite sandwich panel (Meunier *et al.*, 1999).

In
Table **2**, the results obtained from the present theory (IHSAPT) were compared with those obtained from the first model of Frostig, the higher order equivalent single layer theory (HSDT-ESL) and FE modeling in ANSYS code. The results were presented for the first four dimensionless natural frequencies ($\bar{\omega} = \omega a^2 (\rho / E)_c^{1/2} / h$) of a square sandwich panel with $h / a = 0.1$ and $h_c / h = 0.88$. The maximum difference between the present theory and the higher order equivalent single layer theory (FSDT-ESL) was 9.45 percent. Due to core flexibility in the current theory, the obtained natural frequencies from current theory were lower than the natural frequencies obtained from the FSDT-ESL. Also, the present results were in good agreement with those obtained from finite element ANSYS software and the first higher order Frostig's theory. In Table 3, dimensionless natural frequencies of sandwich panel are presented with the material properties given in Table 1 and lay-up sequences [45/-45/45] for the face sheets.

Mode No.	Present model	1st model of Frostig (Rahmani *et al.*, 2009)	Error difference (%)	ANSYS (Rahmani *et al.*, 2009)	Error difference (%)	HSDT-ESL (Meunier *et al.*, 1999)	Error difference (%)
1	14.37	14.27	0.7	14.74	2.57	15.28	6. 33
2	26.53	26.31	0.8	26.83	1.13	28.69	8.14
3	27.17	27.04	0.4	27.53	1.32	30.01	9.45
4	35.24	34.95	0.82	35.60	1.02	38.86	9.27

Table 2: Comparing dimensionless natural frequencies of a flat composite sandwich panel.

As can be seen in Table 3, the results of the present theory were in good agreement with those of IHSAPT (Malekzadeh *et al.* 2005). Considering of different displacement fields for the core layers, there was the discrepancy between the results. In the present theory, displacement field for the core was assumed to be a polynomial with unknown coefficients. But, Nayak *et al.* (2002) and Malekzadeh *et al.* (2005) used equivalent single layer Reddy's theory and 3D elasticity theory for the core, respectively.

Mode No.	Dimensionless natural frequency				
	Present model	IHSAPT (Malekzadeh *et al.*, 2005)	Error difference (%)	FE model (Nayak *et al.*, 2002)	Error difference (%)
1	15.37	15.53	1.04	16.09	4.68
2	27.17	27.36	1.94	28.93	6.47
3	27.17	27.36	0. 6	28.93	6.47
4	36.19	36.93	2.04	38.76	7.1

Table 3: Comparing dimensionless natural frequencies of a flat composite sandwich panel [45/-45/45/core/45/-45/45].

Example 2: Free vibration analysis of an open single curved composite sandwich panel with SSSS B.C.

In this example, free vibration analysis of an open single curved composite sandwich panel with foam core was investigated. Lay-up sequences for face sheets were [0/90]. Mechanical properties of the face sheets and core are given in Table 4.

Foam core	Laminate face sheets
$E_1 = E_2 = E_3 = 6.89\,\mathrm{MPa}$, $G_{12} = G_{13} = G_{23} = 3.45\,\mathrm{MPa}$, $\nu = 0.32,\ \rho = 94.195\,\mathrm{Kg}/\mathrm{m}^3$.	$E_1 = 131$ GPa, $E_2 = E_3 = 10.34\,\mathrm{GPa}$, $G_{12} = G_{13} = 6.895\,\mathrm{GPa}$, $G_{13} = 6.205\,\mathrm{GPa}$, $\nu_{12} = \nu_{13} = 0.22,\ \nu_{23} = 0.49,\ \rho = 1627$ Kg / m^3.

Table 4: Material properties of the single curved composite sandwich panel (Armenakas et al. 1969).

In the Table 5 dimensionless first natural frequency for thin $(h/b = 0.01)$ and thick $(h/b = 0.1)$ sandwich panels with three different ratios of radius to width (R/b) were presented. In this table, results of the present theory (IHSAPT) were compared with those obtained from the first Frostig's model, first order shear deformation theory, higher order equivalent single layer theory and FE modeling in ANSYS code. As can be seen in Table 5, the current results were in good agreement with FE modeling in ANSYS code. Table 5 also shows that results of different theories for the thin sandwich panel were in better agreement with each other than those for the thick sandwich panel.

R/b	h/b	Dimensionless natural frequency: **Present model**	Frostig's 1st model (Rahmani *et al.*, 2009)	Error difference(%)	ANSYS (Rahmani *et al.*, 2009)	Error difference(%)	HSDT-ESL (Armenakas *et al.*, 1969)	Error difference(%)	FSDT-ESL (Armenakas *et al.*, 1969)	Error difference(%)
1	0.01	66.82	63.27	5.31	64.62	3.29	64.64	3.26	64.80	3.02
	0.1	6.77	5.65	16.54	6.46	4.58	7.71	13.88	14.16	109.15
2	0.01	34.95	33.87	3.09	34.50	1.29	35.90	2.72	36.21	3.06
	0.1	3.75	2.96	21.07	3.71	1.07	5.82	55.2	14.026	274.93
3	0.01	24.96	24.17	3.17	24.81	0.60	26.69	6.93	27.12	8.65
	0.1	2.85	2.19	23.15	2.83	0.70	5.37	88.42	14.00	391.22

Table 5: Comparing dimensionless fundamental natural frequency of an open single curved sandwich panel (a/b=1).

Example 3: Free vibration analysis of a flat composite sandwich panel with CCCC B.C.

Now, free vibration analysis of a sandwich panel with laminated face sheets and fully clamp boundary conditions (CCCC B.C.) is studied. There has been few research on free vibration of sandwich structures with CCCC B.C.. Therefore, in order to validate the current results, the sandwich structures were modeled in ABAQUS. This example used mechanical properties, given in Table 1.

At first, convergence of the first five dimensionless natural frequencies was investigated (Table 6). It can be seen from this table that the natural frequencies converged after about 13×13 expressions (m=n=13). Table 6 also shows that the lowest convergence rate of the natural frequencies occurred in the first mode shape.

Convergence	Mode sequence number				
m=n	(1,1)	(1,2)	(2,1)	(2,2)	(1,3)
3	20.41	39.21	42.24	54.17	82.50
5	19.29	31.64	32.44	41.41	45.73
7	18.82	30.34	31.01	39.51	44.12
11	18.39	29.36	29.96	38.14	42.85
13	18.28	29.12	29.71	37.81	42.53
15	18.20	28.95	29.54	37.59	42.29

Table 6: Convergence of dimensionless natural frequencies ($\bar{\omega} = \omega a^2(\rho / E)_c^{1/2} / h$, a=b , a/h=10, h_c/h=0.88, [0/90/0/core/0/90/0]).

In Table 7, the current results were compared with the presented FE model by ABAQUS code and the higher order equivalent single layer theory (HSDT-ESL) presented by Nayak *et al.* (2002). As can be seen in Table 7, the results of the present method were in very good agreement with those of FE model in ABAQUS; but, there was little difference between the current results and those of the HSDT-ESL. It is because the HSDT-ESL model did not consider flexibility of the core layer.

Mode No. (m,n)	Dimensionless natural frequency[0/90/0/core/0/90/0]				
	Present model	ABAQUS	Error difference (%)	(HSDT-ESL) (Nayak *et al.*, 2002)	Error difference (%)
(1,1)	18.20	17.87	-1.85	20.01	-9.94
(1,2)	28.95	28.32	-2.22	32.23	-11.32
(2,1)	29.54	28.92	-2.17	33.34	-12.86
(2,2)	37.59	36.78	-2.15	42.27	-12.45
(1,3)	42.29	41.36	-2.19	48.16	-13.88

Table 7: Comparing dimensionless natural frequency of a flat composite sandwich panel.

Example 4: Free vibration analysis of a composite sandwich cylindrical panel with SSSS B.C.

In this example, free vibration analysis of a composite sandwich cylindrical panel with SSSS B.C. is investigated. Lay-up sequences for face sheets are [0/90/0]. Mechanical properties of the face sheets and core are given in Table 8.

Foam core	Laminate face sheets
$E_1 = E_2 = E_3 = 6.89\,\mathrm{MPa}$, $G_{12} = G_{13} = G_{23} = 6.89\,\mathrm{MPa}$, $\nu = 0,\ \rho = 97\,\mathrm{Kg/m^3}$.	$E_1 = 131$ GPa, $E_2 = E_3 = 10.34\,\mathrm{GPa}$, $G_{12} = G_{13} = 6.895\,\mathrm{GPa}$, $G_{13} = 6.205\,\mathrm{GPa}$, $\nu_{12} = \nu_{13} = 0.22,\ \nu_{23} = 0.49,\ \rho = 1627\ \mathrm{Kg/m^3}$.

Table 8: Material properties of a composite sandwich cylindrical panel.

In

Table **9** the dimensionless first natural frequency of sandwich panels with two different ratios of radius to width are presented. In this table, results of the present theory (IHSAPT) are compared with the three layer theory presented by Rahmani *et al.* (2012) and with the three dimensional elasticity solutions given in Yasin and Kapuria (2012). As can be seen in

Table **9**, the present and Rahmani *et al.* (2012) results show better agreement than Yasin and Kapuria (2012) ones. Because the present paper and Rahmani *et al.* (2012) used the high order sandwich panel theory, while Yasin and Kapuria (2012) used the zig-zag theory.

R/a	Present model	Rahmani *et al.* (2012)	Yasin and Kapuria (2012)
2	3.1236	2.9646	3.5593
5	1.8923	1.7859	2.2664

Table 9: Comparing dimensionless natural frequency of the composite sandwich cylindrical panel.

5 RESULTS

According to the above examples, all formulations of free vibration analysis were validated. Now, some examples are considered and the obtained results are presented and discussed.

Example 1: Free vibration analysis of a double curved composite sandwich panel with SSSS and CCCC B.Cs.

In this example, free vibration analysis of a double curved composite sandwich panel with SSSS and CCCC B.Cs. was investigated. Mechanical and geometrical properties of the sandwich structure are given in Table 10. Lay-up sequences of the top and bottom face sheets were [0/90/0] and the sandwich panel was symmetric about mid-plane.

In Table 11, the dimensionless natural frequencies of the double curved composite sandwich panel for the first four mode shapes with both boundary conditions are presented.

$E_1 = E_2 = E_3 = 0.10363$ GPa, $G_{12} = G_{13} = G_{23} = 0.05$ GPa, $\nu = 0.32$, $\rho = 130$ Kg / m^3.	Foam core
$E_1 = 24.51$ GPa, $E_2 = E_3 = 7.77$ GPa, $G_{12} = G_{13} = 3.34$ GPa, $G_{23} = 1.34$GPa, $\nu_{12} = \nu_{13} = 0.078$, $\nu_{23} = 0.49$, $\rho = 1800$ kg / m^3.	Composite face sheets
$h_c / h = 0.88,\ a = 10h,\ R_{c1} = R_{c2} = 3a,\ a = b.$	Geometric

Table 10: Mechanical and geometrical properties of a double curved composite sandwich panel.

Mode No. (m,n)	$\bar{\omega} = \omega a^2 (\rho / E)_c^{1/2} / h$	
	SSSS B.C.	CCCC B.C.
(1,1)	16.6813	21.7969
(1,2)	27.8385	30.5294
(2,1)	28.6530	31.1720

(2,2)	36.2091	38.7066

Table 11: Dimensionless natural frequencies of a double curved composite sandwich panel.

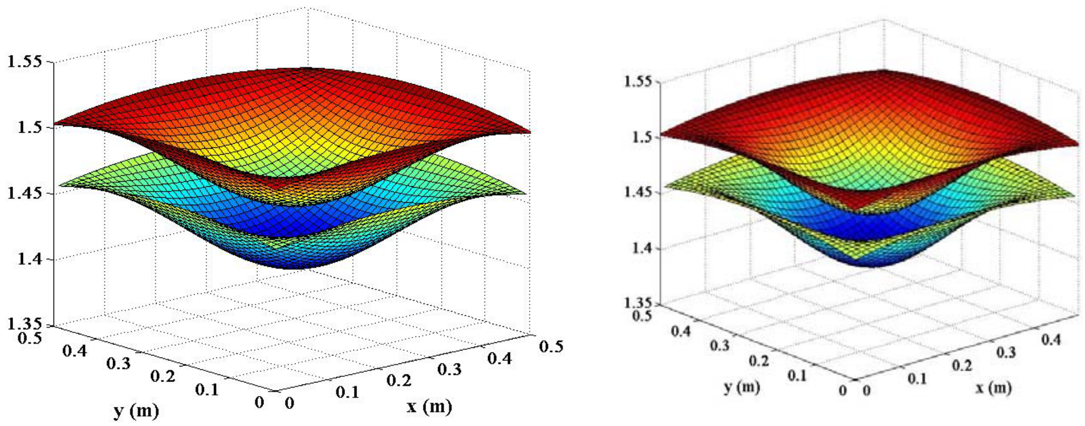

(a) SSSS B.C. (b) CCCC B.C.

Figure 2: Mode shapes of the face sheets at the first natural frequency

for a double curved composite sandwich panel with SSSS and CCCC B.Cs.

As expected, the natural frequencies of the double curved sandwich structures with CCCC B.C. were higher than those with SSSS B.C.. As shown in Table 11, the first dimensionless natural frequency for both boundary conditions occurred in mode shape (m,n)=(1,1). In Figure 2 mode shapes of the face sheets are presented at the first natural frequency for the double curved composite sandwich panel with both boundary conditions.

Example 2: Effects of geometrical parameters and types of boundary conditions on the free vibration analysis of a double curved composite sandwich panel

In this example, effects of various parameters on free vibration response of a double curved composite sandwich panel with SSSS and CCCC B.Cs. were investigated. Properties of the sandwich structure are given in Table 10. Lay-up sequences of the face sheets were [0/90/0] and the sandwich panel was symmetric about the mid-plane.

First, effects of h_c/h (core to panel thickness ratio) and R_1/R_2 (ratio of radii of curvatures) ratios on the first dimensionless natural frequency were studied. It is clear that core to panel thickness ratio and ratio of radii of curvatures had a significant effect on free vibration and dynamic analysis of the sandwich panels. In

Figure 3(a)-(b), effects of h_c/h and R_1/R_2 ratios on the first natural frequency (for both boundary conditions) are shown, respectively. In these figures, length (a) and width (b) of sandwich panel were constant and did not change by thickness of the panel.

It can been seen in

Figure 3(a) that, with increasing core to panel thickness ratio for both boundary conditions, the first dimensionless natural frequency decreased. With increasing h_c/h ratio, the first natural frequency decreased, too. Also, the difference between natural frequencies for SSSS and CCCC B.Cs. at h_c/h=0.1 was higher than that at h_c/h=0.9. In general, with increasing thickness of the core, natural frequencies increased because increasing in the thickness of the core increased stiffness of the sandwich panel.

Figure 3(b) shows that, with increasing R_1/R_2 ratio for both boundary conditions until approximately R_1/R_2 =3, the first natural frequency decreased and converged to a constant value. This behavior occurred due to with increasing R_1/R_2 ratio, geometry of double curve panel converged in the cylindrical single curve panel. In addition, selection of SSSS B.C. for a double curved composite sandwich panel decreased the first dimensionless natural frequency of the panel, as can be seen in Figure 3(b).

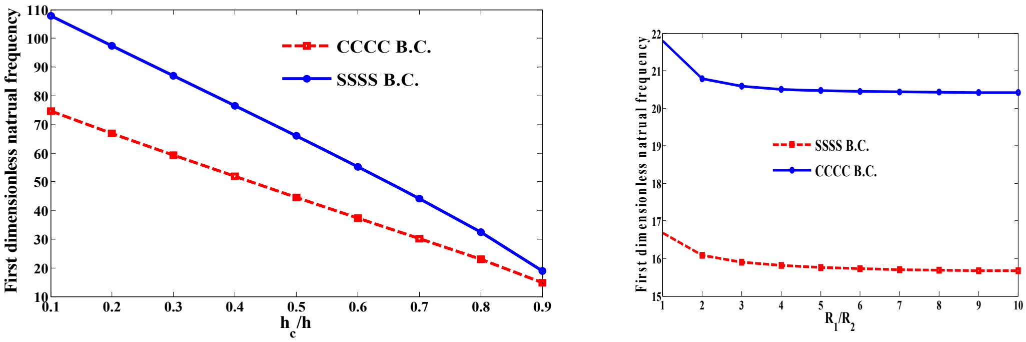

(a) Core to panel thickness ratio (b) Radii of curvatures ratio

Figure 3: Effects of R_1/R_2 and h_c/h ratios on the first dimensionless natural frequency of a double curved composite sandwich panel with both boundary conditions.

Now, effects of fiber angle, i.e. lay-up sequence and type of boundary condition, on the first natural frequency are investigated. In Figure 4 (a)-(b), variations of the first natural frequency with fiber angle for a sandwich panel with SSSS and CCCC B.Cs. are presented, respectively.

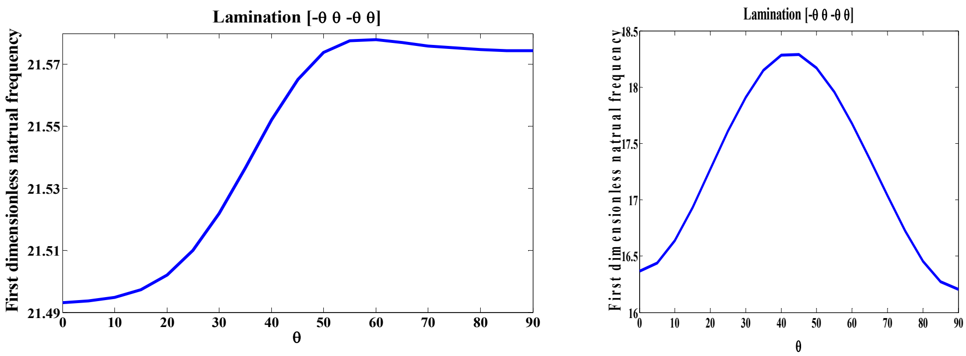

(a) SSSS B.C. (b) CCCC B.C.

Figure 4: Effect of composite lay-up sequence on the first dimensionless natural frequency of a double curved composite sandwich panel with a. SSSS B.C. and b. CCCC B.C.

As can be seen in Figure 4(a), maximum first natural frequency for SSSS B.C. occurred in fiber angle 45 ° while Figure 4(b) shows that maximum first natural frequency for CCCC B.C. approximately occurred in fiber angle 55 ° . In addition, natural frequency of a double curved composite panel with CCCC B.C. for all fiber angles was more than that with SSSS B.C..

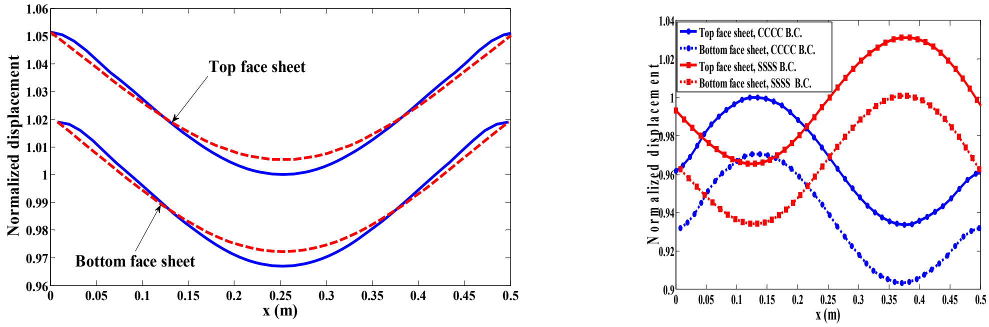

(a) First shape mode (b) Second shape mode

Figure 5: Normalized displacements of the face sheets for a double curved composite sandwich panel with SSSS and CCCC B.Cs. corresponding to the first and second mode shapes.

The normalized modal displacements corresponding to the first and second natural frequencies for a sandwich panel with SSSS and CCCC B.Cs. are shown in
Figure 5, where amplitudes of the vibration in this figure are normalized. As is obvious in
Figure 5(a), normalized displacements of the top face sheet was higher than those of the bottom face sheet for both boundary conditions. In this figure, the dot lines belong to CCCC B.C.. In the first mode shape, the top and bottom face sheets moved vertically in the same direction for SSSS and CCCC B.Cs. while
Figure 5(b) shows that the top and bottom face sheets in the second mode shape with SSSS B.C. moved in the opposite direction those with CCCC B.C..

6 CONCLUSION

In this work, free vibration analysis of double curved composite sandwich panels with simply support and fully clamped boundary conditions was studied. The analysis was very general and valid for any type of core, any type of face sheets as well as the cases in which the conditions at the upper face sheet were different from those at the lower one along the same edge. Thickness of the upper face sheet might be different from that of the lower face sheet. Transverse shear and rotary inertia effects of face sheets were taken into consideration. Therefore, the upper and lower face sheets could be thick or thin, independent from each other.

The numerical study revealed that soft-core sandwich panels exhibited a complex behavior and vibration patterns of the sandwich panels were more complex than those of the homogeneous panels. The thicker panels with a thicker core provided greater resistance to resonant vibrations. The effect of types of boundary conditions, core to panel thickness ratio, ratio of radii curvature and fiber angle on dynamic response of double curved composite sandwich panels was also studied.

The results revealed that:

1. The present theory for free vibration analysis of double curved thick sandwich panels was more accurate than other theories.
2. By increasing the core to panel thickness ratio, the first natural frequency of double curved composite sandwich panels for SS and CC B.Cs. linearly decreased.
3. By increasing the radii of curvatures ratio until approximately $R_1/R_2 = 3$, the first natural frequency of double curved composite sandwich panels for SS and CC B.Cs. decreased and after that converged to a constant value..
4. Maximum first natural frequency for SSSS B.C. occurred in fiber angle 45° while maximum first natural frequency for CCCC B.C. approximately occurred in fiber angle 55°.

References

Armenakas, A.E., Gazis, D.C., Herrmann, G. (1969). Free vibrations of circular cylindrical shells. Oxford: Pergamon Press.

Awrejcewicz, J., Kurpa, L., Shmatko, T. (2013). Large amplitude free vibration of orthotropic shallow shells of complex shapes with variable thickness. Latin American Journal of Solids and Structures 10: 149–162.

Bhimaraddi, A. (1993). Three-dimensional elasticity solution for static response of orthotropic doubly curved shallow shells on rectangular planform. Composite Structures 24: 67–77.

Biglari, H., Jafari, A.A. (2010a). Static and free vibration analyses of doubly curved composite sandwich panels with soft core based on a new three-layered mixed theory. Journal of Mechanical Engineering Science 224: 2332–2349.

Biglari, H., Jafari, A.A. (2010b). High-order free vibrations of doubly-curved sandwich panels with flexible core based on a refined three-layered theory. Composite Structures 92: 2685–2694.

Cetkovic, M.D., Vuksanovic, j. (2009). Bending, free vibrations and buckling of laminated composite and sandwich plates using a layerwise displacement model. Composite Structures 88: 219–227.

Frostig, Y., Baruch, M. (1994). Free vibration of sandwich beams with a transversely flexible core: a high order approach. Journal of Sound and Vibration 176(2): 195–208.

Frostig, Y., Thomsen, O.T. (2004). Higher-order free vibration of sandwich panels with a flexible core. International Journal of Solids and Structures 41: 1697–1724.

Garg, A.K., Kharem, R.K. and Kant, T. (2006), "Higher-order closed-form solutions for free vibration of laminated composite and sandwich shells", J. Sandw. Struct. Mater., 8, 205–235.

Ghavanloo, E., Fazelzadeh, S.A. (2013). Free vibration analysis of orthotropic doubly-curved shallow shells based on the gradient elasticity. Composites Part B: Engineering 45(1): 1448–1457.

Ghugal, Y.M., Sayyad, A.S. (2011). Free vibration of thick orthotropic plates using trigonometric shear deformation theory. Latin American Journal of Solids and Structures 8: 229 – 243.

Kant, T., Patil, H.S. (1991). Buckling load of sandwich columns with a higher-order theory. Journal of Reinforced Plastics and Composites 10(l): 102–109.

Kapuria, S., Bhattacharyya, M., Kumar, A.N. (2008). Bending and free vibration response of layered functionally graded beams: a theoretical model and its experimental validation. Composite Structures 82: 390–402.

Khalili S.M.R., Rahmani O., Malekzadeh F. K., Thomsen O.T. (2014). High-order modelling of circular cylindrical composite sandwich shells with a transversely compliant core subjected to low velocity impact. Mechanics of Advanced Materials and Structures 21(8): 680–695.

Li, Q., Iu, V.P., Kou, K.P. (2008). Three-dimensional vibration analysis of functionally graded material sandwich plates. Journal of Sound and Vibration 311: 498–515.

Malekzadeh, K., Khalili, M.R., Mittal, R.K. (2005). Local and global damped vibrations of plates with a viscoelastic soft flexible core: an improved high-order approach. Journal of Sandwich Structures and Materials 7: 431-456.

Malekzadeh, K., Khalili, M.R., Olsson, R., Jafari A. (2006). Higher-order dynamic response of composite sandwich panels with flexible core under simultaneous low-velocity impacts of multiple small masses. International Journal of Solids and Structures 43: 6667–6687.

Malekzadeh, K., Mozafari, A., Ashenai Ghasemi, F. (2014). Free Vibration Response of a Multilayer Smart Hybrid Composite Plate with Embedded SMA Wires. Latin American Journal of Solids and Structures 11: 279–298.

Meunier, M., Shenoi, R.A. (1999). Free vibration analysis of composite sandwich plates. Journal of Mechanical Engineering Science 213(7): 715–727.

Mochida, Y., Ilanko, S., Duke, M., Narita, Y. (2012). Free vibration analysis of doubly curved shallow shells using the superposition-Galerkin method. Journal of Sound and Vibration 331: 1413–1425.

Nayak, A.K., Shenai, R.A., Moy, S.S.J. (2002). Analysis of damped composite sandwich plates using plate bending element with substitute shear strain fields based on Reddy's higher-order theory. Journal of Mechanical Engineering Science 216: 591–606.

Rafieipour, H., Lotfavar, A., Masroori, A., Mahmoodi, E. (2013). Application of Laplace Iteration method to Study of Nonlinear Vibration of laminated composite plates. Latin American Journal of Solids and Structures 10: 781–795.

Rahmani, O., Khalili, S.M.R., Malekzadeh, K. (2009). Free vibration response of composite sandwich cylindrical shell with flexible core. Composite Structures 92: 1269–1281.

Rahmani, O., Khalili, S.M.R., Thomsen, O.T. (2012). A high-order theory for the analysis of circular cylindrical composite sandwich shells with transversely compliant core subjected to external loads. Composite Structures 94: 2129–2142.

Reddy, J.N. (2003). Mechanics of Laminated Composite Plates and Shells: Theory and Analysis, (2th Edition), CRC Press, Texas, USA.

Singh, A.V. (1999). Free vibration analysis of deep doubly curved sandwich panels. Composite Structures 73: 385–394.

Viola, E., Tornabene, F., Fantuzzi N. (2013). General higher-order shear deformation theories for the free vibration analysis of completely doubly-curved laminated shells and panels. Composite Structures 95: 639–666.

Yasin, M.Y., Kapuria, S. (2013). An efficient layerwise finite element for shallow composite and sandwich shells. Composite Structures 98: 202–214.

Zenkour, A.M. (2005a). A comprehensive analysis of functionally graded sandwich plates: part 1 – deflection and stresses. International Journal of Solids and Structures 42: 5224–5242.

Zenkour, A.M. (2005b). A comprehensive analysis of functionally graded sandwich plates: part 2 – deflection and stresses. International Journal of Solids and Structures 42: 5224–5242.